The Voltage-Pulsing Effects in AC Plasma Display Panel

Young Kyo Shin, Chae Hwa Shon, Woong Kim, and Jae Koo Lee

***Abstract*—The effect of the voltage pulsing is simulated in ac plasma display panel using various two-dimensional simulation codes. The volume-averaged density increases rapidly because of the large electric field in the ac-plasma display panel cell as the peak voltage is raised. The ignition time and the decaying time of the discharge are related to the external voltage. The space and time variations of the charged particle densities and the potential profile are described for various voltage forms. The ion energy distribution near the cathode-side dielectric which plays an important role in the MgO lifetime and the secondary electron emission coefficient is concentrated to much lower energies than the applied voltage.**

***Index Terms*—Gas discharge, plasma display panel.**

I. Introduction

PLASMA display panel (PDP) is one of the most promising candidates for high definition color television (HDTV) [1]. The PDP is based on the use of the light emitted by the gas discharge whose pressure is a few hundred torr in the few hundred μm range. There is considerable attention in enhancing the luminance efficiency of PDP for HDTV. The cell optimization, the gas composition, and the voltage pulse characteristics are studied to improve the PDP efficiency. It is difficult to measure the physical quantities such as the density and the temperature directly because of the small size of the PDP cell. Computer simulation of PDP cell has become a useful tool to understand the discharge characteristics in the cell. Sahni and Lanza investigated the importance of the dependence of the secondary emission coefficient on E/P for a neon-based PDP [2]–[3]. Drallos developed one-dimensional (1-D) kinetic PDP model [4] and an analytic approach [5]. A number of the simulations have investigated PDP cell dynamics [6]–[11]. Most simulations employ fluid approaches. Meunier [7] showed the diagram indicating the dissipation of energy by the electrons and the ions in the discharge using 1-D neon-xenon based model. Punset [8] shows the electrical interaction between the adjacent cells and the effects of electrode misalignment.

In an ac-PDP, the charge accumulations on the dielectric turn off the discharge when the gap voltage is below the breakdown voltage. Using the self-extinguishing of an ac-PDP cell, we vary the applied voltage and the pulse length keeping their product constant for various voltage forms. The resulting voltage-pulsing effect, the discharge ignition time, the plasma density, and the decay time of the density are examined using two-dimensional (2-D) fluid model; the ion energy distribution near the dielectric is calculated using a kinetic code OOPIC [12].

Manuscript received November 12, 1998; revised May 7, 1999. This work was supported in part by the PDP Research Center, the BSRI-Special Fund of POSTECH, and the Basic Science Research Institute Program, Ministry of Education, Project 97-2439.

The authors are with the Department of Physics, Pohang University of Science and Technology, Pohang 790-784, South Korea (jkl@postech.ac.kr).

Publisher Item Identifier S 0093-3813(99)08123-0.

II. Numerical Method

A. Fluid Equation

The fluid model is used to simulate the PDP cell shown in Fig. 1(a). The model consists of a set of fluid equations for electrons and ions, Poisson's equation for the electric field, and the appropriate boundary conditions. The model equations [13] are written as

$$\frac{\partial n_e}{\partial t} + \nabla \cdot \boldsymbol{\Gamma}_e = K_{iz} n_e N - \alpha n_e n_p \tag{1}$$

$$\frac{\partial n_p}{\partial t} + \nabla \cdot \boldsymbol{\Gamma}_p = K_{iz} n_e N - \alpha n_e n_p \tag{2}$$

$$\nabla \cdot (\epsilon \nabla V) = -e(n_p - n_e) \tag{3}$$

$$\boldsymbol{\Gamma}_e = -D_e \nabla n_e - n_e \mu_e \boldsymbol{E} \tag{4}$$

$$\boldsymbol{\Gamma}_p = -D_p \nabla n_p + n_p \mu_p \boldsymbol{E}. \tag{5}$$

Equations (1) and (2) are the continuity equations of electron and ion, respectively. $n_{p,e}$, $D_{p,e}$, and $\mu_{p,e}$ are the density, the diffusion, and the mobility of electron (ion), respectively. ϵ, K_{iz}, N, and α are the permittivity, the ionization rate constant, neutral density, and the recombination efficient, respectively.

The first two moments of Boltzmann equation are used to describe the electron and ion transport phenomena. The equation of motions for the plasma particle are replaced by (4) and (5) assuming an equilibrium with the local electric field at a given location and time. The ionization source and mobility $\mu_{p,e}$ are the function of the reduced electric field E/P obtained from the space-averaged Boltzmann equation.[1] E is the electric field and P is the neutral gas pressure. Diffusion coefficients $D_{p,e}$ are obtained from the Einstein relation. We assumed the electron temperature of 4 eV.

The simulation domain as in Fig. 1(a) corresponds to a 2-D Cartesian geometry. The z direction perpendicular to the plane of Fig. 1(a) is assumed to be infinite. The equations are discretized by the finite difference method for the spatial derivatives, while the time derivatives are discretized by forward time. The continuity equations and Poisson's equation

[1]The Siglo Data base, CPAT and Kinema Software, http://www.csn.net/siglo (1998).

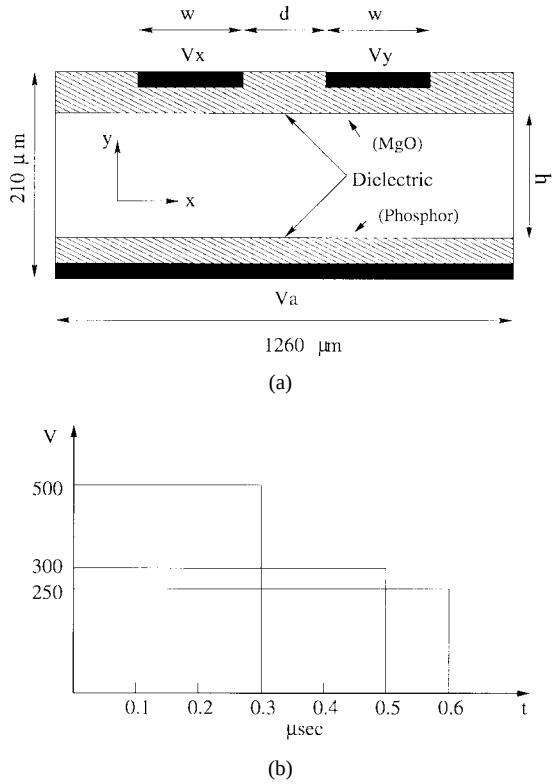

Fig. 1. (a) Schematic of the simulated geometry. Instead of inserting MgO and phosphor into the simulation domain, MgO and phosphor are considered with γ_{se} of the dielectric layer. (b) Voltage-pulse form applied to the scan electrode V_x.

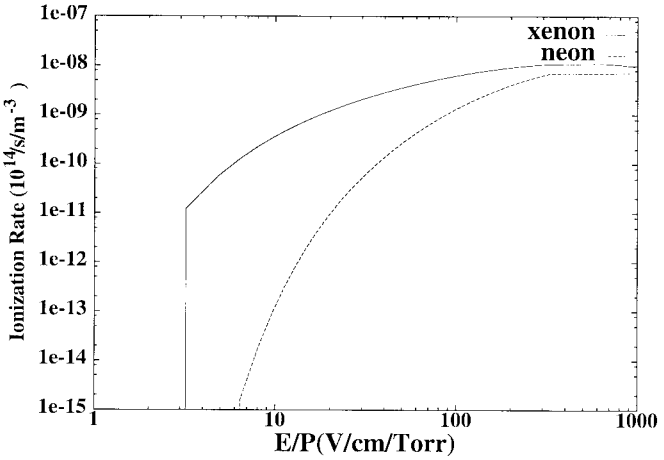

Fig. 2. Ionization rate of neon (dashed line)-xenon (solid line) (90/10%) mixture gas as a function of electric field.

can be written in a matrix form using the five-point formula in two dimension [14]

$$a_{ij}u_{i+1,j} + b_{ij}u_{i-1,j} + c_{ij}u_{i,j+1} + d_{ij}u_{i,j-1} + e_{ij}u_{ij} = f_{ij}.$$

Poisson's equation is solved by the successive overrelaxation method [14], [15] until convergent solution is obtained. The continuity equations are solved by the alternate direction implicit (ADI) [15]. The implicit method is performed in the continuity equations to avoid the Courant–Friedrichs–Lewy (CFL) stability criterion [15]. The exponential scheme proposed by Sharfetter and Gummel [16] is used to solve the flux equations. The principal advantage of this exponential scheme is that it provides numerical stability of the flux under all conditions. Neumann boundary condition is employed on the side boundaries. The normal electric field and normal density gradient on the side boundary are zero. The normal flux which is the sum of these two values becomes zero on the side boundaries. There are two boundary conditions at the plasma-dielectric interfaces; the flux boundary in front of the dielectric layer and the charge accumulation on the dielectric surfaces. At the interfaces between the gas and the dielectric surfaces, the surface charge density is calculated by integrating the charged particle fluxes to the surfaces during the discharge evolution. The charged particle fluxes to a dielectric surface is as follows:

$$\boldsymbol{\Gamma}_p = n_p\mu_p E + 0.25 n_p v_{th_p} \tag{6}$$

$$\boldsymbol{\Gamma}_e = n_e\mu_e E + 0.25 n_e v_{th_e} - \gamma_{se}\boldsymbol{\Gamma}_p \tag{7}$$

where $n_{p,e}$, $v_{th_{p,e}}$, and γ_{se} are the charged particle density at the dielectric surface, thermal velocity, and secondary electron emission coefficient due to the ion bombardment, respectively.

The boundary condition of the surface charging equation at the interface between the dielectric surfaces and the gas gap is as follows:

$$(\epsilon_0\boldsymbol{E}_0 - \epsilon_1\boldsymbol{E}_1)\cdot\boldsymbol{n}_s = \sigma \tag{8}$$

where σ is the time integrated charge density on the dielectric surface, $\boldsymbol{E}_0$ and $\boldsymbol{E}_1$ are the electric field in the gas and at the dielectric surface, $\boldsymbol{n}_s$ is the unit vector perpendicular to the dielectric surface.

B. Kinetic Simulation

Fluid simulations employ only the quantities averaged over velocity distribution, thus having limitation in examining the kinetic phenomena inside the cell. Kinetic phenomena occur in the sheath whose size is considerable compared with the cell size. Kinetic simulation has a unique capability to calculate the energy distributions, which are important to understand the characteristics of the PDP cell. The incident ion energy toward the dielectric is related to the lifetime of PDP. The impact due to ions having high energy on the protective layer such as dielectric and MgO is large and reduces the lifetime of devices. We investigate the ion energy distribution in front of the dielectric layer varying the applied voltage.

Kinetic simulation calculates the ion current density by integrating the distribution function over the velocity space. For our ac-PDP, we use OOPIC [12] code which is 2-D particle code using particle in cell/Monte-Carlo (PIC-MC) collision.

III. Simulation Results with Various Pulse Shapes

A. Geometry, Initial Conditions, and Voltage Forms

The cell geometry is shown in Fig. 1(a). The cell width and height are 1260 μm, 210 μm, respectively. The distance d between the scan V_x and the common V_y electrodes is set to 160 μm in the typical case. The distance between the dielectric layers is h, which affects the ignition of the cell. A large h

increases the luminance efficiency if the positive column is used. The product of the neutral gas pressure and the large h needs the high voltage to turn on the cell. The neutral gas is a neon-xenon (90/10%) mixture with the gas pressure 500 torr. Fig. 1(b) shows the three external voltage forms applied to the V_x electrode. Molecular ions are not taken into account in the simulation. The cell is ignited when the voltage is applied to the V_x and V_a electrodes. After cell ignition, the cell is sustained with the V_x and V_y electrodes. We concern the first stage of the cell ignition. The external voltage 250 V is applied to the V_x electrode. The V_y and the V_a electrodes are grounded. This type is similar to the matrix geometry because the discharge between the V_x and the V_y electrodes do not occur with the distance $d = 160$ μm. The dielectric layers of 30 μm are deposited above the electrodes, the dielectric constant is ten. The charge accumulation on the dielectric layer counteracts the external voltage and turns off the discharge after the maximum current flows into the dielectric surface. MgO has a large secondary-electron emission coefficient γ_{se}. Instead of inserting MgO and phosphor into the simulation domain, we consider MgO and phosphor effect with γ_{se} of the dielectric layers. We use the same γ_{se} for MgO and phosphor. We use $\gamma_{se} = 0.5$ and 0.05 for neon and xenon, respectively. The ionization rate of neon-xenon (90/10%) gas is shown in Fig. 2 as a function of E/P. We use the initial plasma density with 10^7 cm^{-3} as in [17].

The products of the applied time and the voltage, which is the area of the curve, are the same in three cases. The similar pulse form is carried by Lieberman and Ashida [18], using the global model to simulate the pulse-power-modulated high-density low-pressure discharge. The plasma density and the electron temperature are increased with the decreasing duty ratio for the same time-averaged power.

B. Discharge Evolution

In the high pressure and the small gap size as in PDP, the voltage is applied to the cell to accelerate electrons toward the anode electrode and to expel them rapidly from the cell because of their light mass and high mobility. The electron loss makes the cell ion-rich. The remaining ions are accelerated toward the cathode electrode to charge the cathode-side dielectric layer. The secondary-emitted electrons due to the ion bombardment are accelerated through the sheath and ionize the neutral gas. The created electron ionizes the neutral gas before exiting from the cell. For 450 ns at 250 V, this process is repeated without increasing the electron density because of their high mobility. The density difference between the electron and the ion is increased with time. After a certain ion density is reached, the space ions create the potential to prevent the electrons from flowing out of the cell as the solid line shown in Fig. 3. The electrons remain in front of the anode dielectric. The electron-increase accomplishes the charge neutrality which makes the flat potential region. As the discharge proceeds, the flat potential region advances toward the cathode dielectric layer as the dashed line shown in Fig. 3.

The charge accumulation on the dielectric layer decreases the external voltage and the discharge extinguishes if the gap voltage is below the breakdown voltage. The dashed line shown in Fig. 3 indicates the potential profile along the direction advancing discharge at the density-peak time. The potential profile after the discharge extinguishes is shown as the dotted line in Fig. 3. The plasma potential between the gas gap is set up to maintain the ambipolar diffusion in the cell.

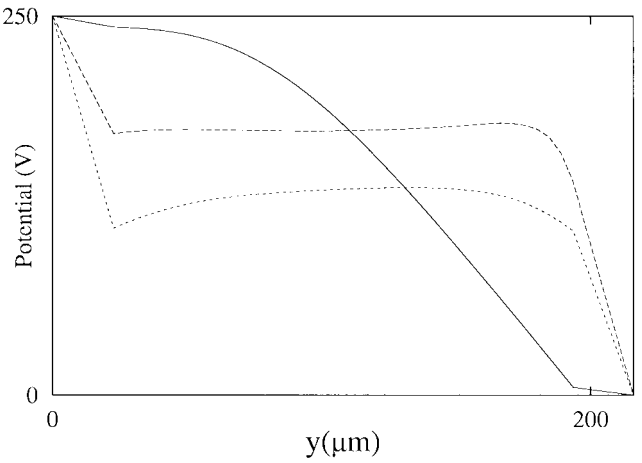

Fig. 3. The potential profiles at three different times along the y direction at the center of V_s electrode for solid (ignition), dash (peak), and dots (after the discharge extinguishes).

C. Voltage-Pulsing Effects

Fig. 4 shows the volume-averaged electron density and the peak value of E/P with time. The discharges for three external voltage forms extinguish within the applied voltage pulse. The discharge is delayed with the decreasing external voltage shown in Fig. 4(a). The ignition time of the discharge is strongly related to the ion flux on the cathode-side dielectric. The ion flux consists of the difference of the drift which is the product of the mobility and the electric and the density gradient term shown in (5). At the initial stage of the discharge, the ion density gradient is very small due to the uniform distribution and the low density. The initial stage is mobility-dominant, the ion flux is affected by the drift term. The increase of the external voltage increases the electric field in the cell and the ion flux. The increased ion flux enhances the dielectric charging at the cathode side. The emitted electrons per unit time are increased, which distorts the potential rapidly.

The peaks of the volume-averaged electron density are 7.81 $\times$ 10^{11}, 1.47 $\times$ 10^{12}, and 8.30 $\times$ 10^{12} cm^{-3} for 250, 300, and 500 V, respectively. The voltage-rise increases considerably the average electron density. Unlike the low voltage such as 250 V, the high voltage of 500 V has large ionization rate in the initial stage and large E/P shown in Fig. 4(b). Although the maximum ionization rate shown in Fig. 2 is reached for 250 V, the E/P range from 200–900 (V/cm/torr) in the case of 500 V extends over the high ionization region. The rapid increase of E/P dose not allow the electron to flow out of the cell. Therefore, we can obtain the high density plasma by increasing the voltage with the same input power. For example, the electron density doubles by increasing by 20% of the external voltage as the dotted line shown in Fig. 4(a).

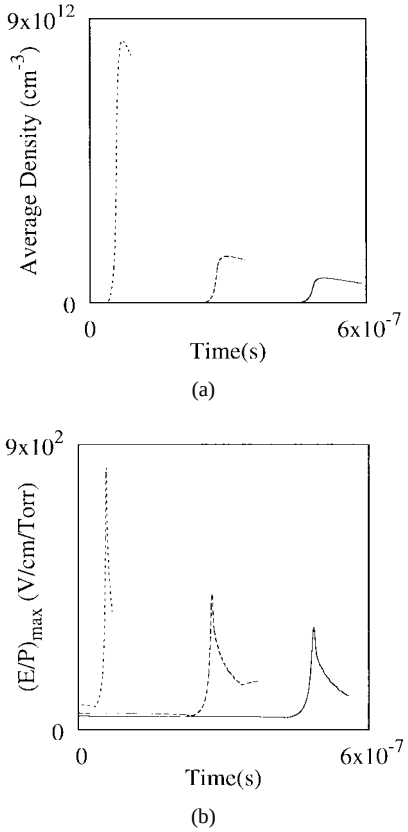

Fig. 4. Time evolutions of (a) the volume-averaged electron densities and (b) the time traces of the maximum E/N for three different external voltages, 250 V (solid), 300 V (dashed), and 500 V (dotted).

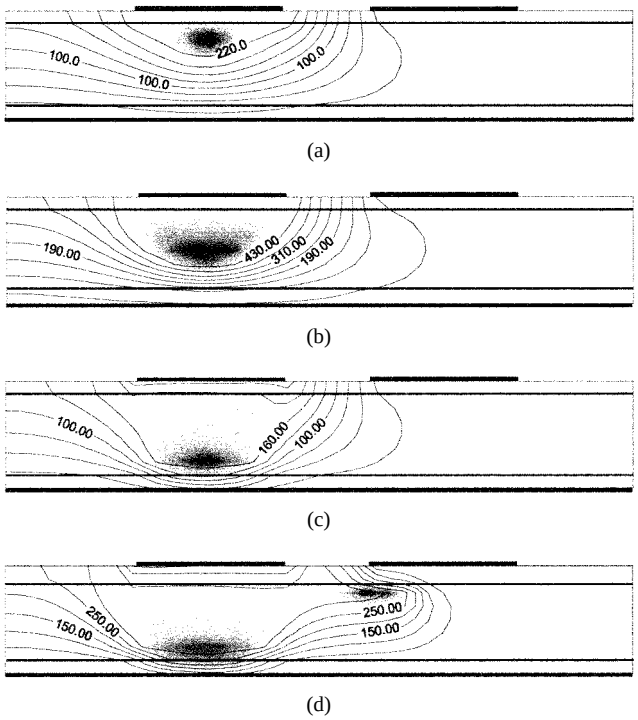

Fig. 5. Contour plots of the electron density and potential: (a) and (b) for the electron density and potential profiles for 250 and 500 V at the ignition of the discharge, respectively. (c) and (d) for the electron density and potential profiles for 250 and 500 at the density peak time.

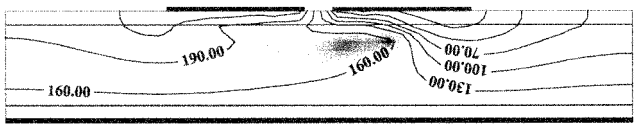

Fig. 6. Contour plots of electron density and potential in the coplanar geometry for 250 V at the density peak time.

After the density peak, due to the charge accumulation on the dielectric surface, the discharge extinguishes. The decrease of the density is slow with a decreasing voltage. Unlike the initial stage, with the discharge extinguished, the potential in the cell is nearly zero. The flux has the diffusion-dominant form due to the density gradient. The high densities produced by the high voltage create the large density gradient than the low voltage toward both dielectric layer. The density gradient makes the density profile parabolic.

Fig. 5(a) and (b) shows the electron density and the potential at the ignition time of the discharge for 250 and 500 V, respectively. The charged particles are produced near the V_x electrode. The flat potential which accomplishes the charge neutrality is shown near the upper dielectric. Fig. 5(c) and (d) show the electron density and the potential at the peak time of the density for 250 and 500 V, respectively. Unlike Fig. 5(c), the strong electric field produces the auxiliary discharge between the V_x and V_y electrodes shown in Fig. 5(d). The sheath size is decreased with the increased voltage.

D. Coplanar Geometry

The electron density and the potential profile in the coplanar geometry at the peak time of the density are shown in Fig. 6. The discharge occurs between V_x and V_y electrodes, V_a is applied to the half of V_x voltage to prevent the discharge between V_x and V_a electrodes and to consider the wall voltage on V_a electrode approximately. The d distance between the adjacent electrodes is 60 μm. h is the same as the previous case. The maximum E/P 199 (V/cm/torr) is smaller than for the case of Section III-C because the large electric field exists inside the dielectric and dose not participate in the ionization. The electron density has a peak near the dielectric above the top electrodes in shown Fig. 6. The xenon excited state Xe* is proportional to the electron density. The phosphor is located over the V_a electrode. The coplanar type has the defect that the density peak is away from the the phosphor.

E. Kinetic Simulation

We use the pure neon gas in the particle simulation using OOPIC [12] to obtain the velocity distribution. Other parameters except for the gas are the same as the fluid simulation. Fig. 7 shows the y component of neon velocity along the y direction in the cell. The energetic neon ions are mainly distributed at the cathode region. The ions in the bulk are in equilibrium with neutral atoms. The particle distribution in front of the cathode dielectric yields the information of the incident ion current-density which plays an important role in the erosion rate and the secondary electron emission at the dielectric surface. OOPIC calculates the particle position and velocity at any time. The velocity distribution is redistributed

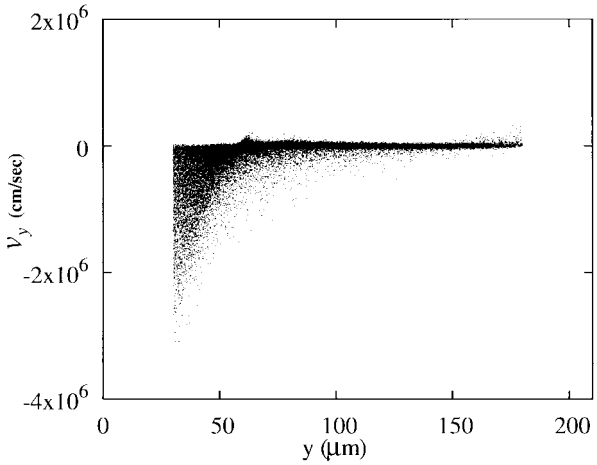

Fig. 7. Phase space : y component of neon velocity along the y direction.

at any time unlike the fluid model which uses the assumed distribution. The energy distribution shown in Fig. 8 is obtained by plotting the particles energies as the x axis and the particle number existing in the small region Δy along the y direction of the cell as the y axis. Ion energy distributions are plotted in a semi-log scale with the energy indicated in x axis. The ion energy distribution function at the number peak for 250 V is shown in Fig. 8(a). The interesting region is a few μm away from the cathode dielectric surface. Fig. 8(a) shows that the majority (90%) of the ions have the energy at or below 10% of the applied voltage of 250 V. The cause of the low ion energy is the frequent elastic collision with the neutral gas and the potential drop between the gap due to the charge accumulation [19]. Fig. 8(b) is the ion energy distribution with the external voltage of 400 V. In spite of the high external voltage, the majority of the ions have energies below 10% of 400 V. The majority of the low ion-energy are below 1–2 eV because of the charge transfer collision with the neutral. The charge-exchange collision reduces the ion velocity. In contrast, for a magnetron discharge, the gas pressure is a few mtorr to make the system collisionless, where the ions in the cathode region are accelerated to several hundred volts, which is 80–90% of the applied voltage [20]. Various other methods such as the modest-energy electron beam [21]–[23] can be used to enhance the plasma densities in a capacitively coupled plasma such as PDP.

IV. Conclusion

The discharge evolution in a PDP cell for various types of pulse shapes is investigated. A small increase in the peak value of the external voltage produces several times larger plasma density. The large E/P range sweeping the maximum ionization rate and the rapid increase in ionization due to the high voltage produce the plasma particles efficiently and rapidly. The density gradient increases due to the high density as the peak voltage is raised. The coplanar type has the low density because the strong electric field exists inside the dielectric. Most charged particles exist near the top electrodes, responsible for the low efficiency because the phosphor is far away from the density peak. The ion energy near the dielectric surface is much lower than the applied voltage due to the elastic collision with the neutral atom and the charge accumulation on the surface. The low ion energy affects the lifetime of MgO layer and the secondary electron emission-coefficient.

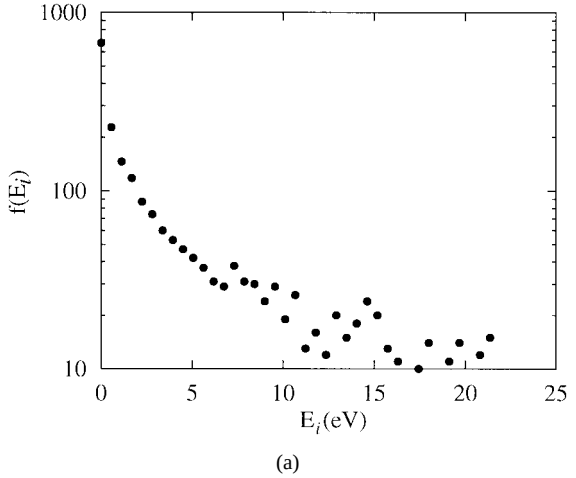

(a)

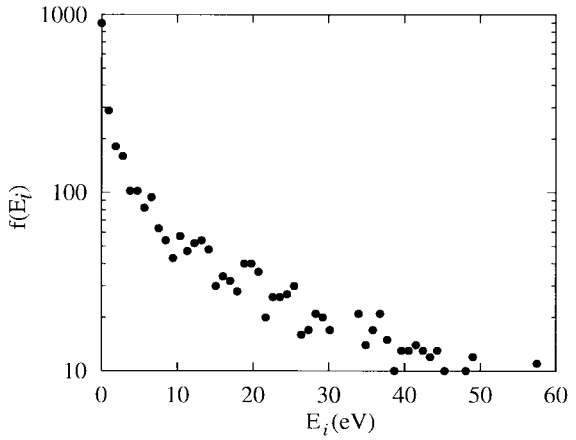

(b)

Fig. 8. Ion energy distributions at the density peak for (a) the external voltage of 250 V and for (b) 400 V. The region between 30–35 μm is calculated.

References

[1] A. Sobel, ''Plasma displays,'' *IEEE Trans. Plasma Sci.*, vol 19, pp. 1032–1047 Dec. 1991.

[2] O. Sahni and C. Lanza, ''Importance of the dependence of the secondary electron emission coefficient on E/P_0 for Paschen breakdown curves in ac plasma panels,'' *J. Appl. Phys.* vol. 47, pp. 1337–1340, Apr. 1976.

[3] O. Sahni, C. Lanza, and W.E. Howard, ''One-dimensional numerical simulation of ac discharges in a high-pressure mixture of Ne+0.1% Ar confined to a narrow gap between insulated metal electrode,'' *J. Appl. Phys.*, vol. 49, pp. 2365–2375, Apr. 1978.

[4] P. J. Drallos, V. P. Nagorny, and W. Williamson, Jr., ''A Kinetic study of the local field approximation in simulations of AC plasma display panels,'' *Plasma Sources Sci. Technol.*, vol. 4, pp. 576–590, 1995.

[5] V. P. Nagorny, P. J. Drallos, and W. Williamson, Jr., ''The dynamics of a high-pressure ac gas discharge between dielectric coated electrode near breakdown threshold,'' *J. Appl. Phys.*, vol. 77, pp. 3645–3656, 1995.

[6] R. Veerasingam, R. B. Campbell, and R. T. MacGrath, '' One-dimensional fluid simulations of a helium-xenon filled ac color plasma flat panel display pixel," *Plasma Sources Sci. Technol.*, vol 6, pp. 157–169, 1997.

[7] J. Meunier, P. Belenguer, and J. P. Boeuf, ''Numerical model of an ac plasma display panel cell in neon-xenon mixtures,'' *J. Appl. Phys.*, vol. 78, pp. 731–745 July 1995.

[8] C. Punset, J. P. Boeuf, and L. C. Pitchford, ''Two-dimensional simulation of an alternating current matrix plasma display cell: Cross-talk and other geometric effects,'' *J. Appl. Phys.*, vol. 83, pp. 1884–1897, 1998.
[9] R. B. Campbell, R. Veerasingam, and R. T. McGrath, '' A two-dimensional multispecies fluid model of the plasma in an AC plasma display panel,'' *IEEE Trans. Plasma Sci.*, vol 23, pp. 698–708, Aug. 1995.
[10] K. C. Choi and K. W. Whang, ''Numerical analysis of the microdischarge in a DC plasma display panel by 2-dimensional multifluid equations,'' *IEEE Trans. Plasma Sci.*, vol. 23, pp. 399–404 June 1995.
[11] K. Takahashi, S. Hashiguchi, Y. Murakami, *et al.*, '' Investigation of discharge phenomena in a cell of color plasma display panel I. one-dimensional model and numerical method,'' *Jpn. J. Appl. Phys.*, vol. 35, pp. 251–258 Jan. 1996.
[12] J. P. Verboncoeur, A. B. Langdon, and N. T. Gladd, ''An object-oriented electromagnetic PIC code,'' *Comp. Phys. Commun.*, vol. 87, pp. 199–211, 1995.
[13] J. K. Lee, L. Meng, Y. K. Shin, H. J. Lee, and T. H. Chung, ''Modeling and simulation of a large-area plasma source,'' *Jpn. J. Appl. Phys.* vol 36, pp. 5714–5723 Sept. 1997.
[14] J. C. Tannehill, D. A. Anderson, and R. H. Pletcher, *Computational Fluid Mechanics and Heat Transfer*. Washington, DC: Taylor & Francis, 1997.
[15] W. H. Press, S. A. Teukolsky, W. T. Vetterling, and B. P. Flannery, *Numerical Recipes in C.* Cambridge, U.K.: Cambridge Univ. Press, 1992.
[16] D. L. Sharfetter and H. K. Gummel, ''Large-signal analysis of a silicon read diode oscillator,'' *IEEE Trans. Electron Devices*, vol 16, pp. 64–77, 1967.
[17] Y. K. Shin, J. K. Lee, and C. H. Shon, ''Two-dimensional breakdown characteristics of PDP cells for varying geometry,'' *IEEE Trans. Plasma Sci.*, vol. 27, pp. 14–15, Feb. 1999.
[18] M. A. Lieberman and S. Ashida, ''Global model of pulse-power-modulated high-density, low-pressure discharges,'' *Plasma Sources Sci. Technol.*, vol 5, pp. 145–158, 1996.
[19] Y. K. Shin, J. K. Lee, C. H. Shon, and W. Kim, "Ion energy distribution in alternating-current plasma display panel cell,'' *Jpn. J. Appl. Phys.*, vol. 38, pp. L174–L177, 1999.
[20] C. H. Shon, J. K. Lee, H. J. Lee, Y. K. Shin, Y. Yang, and T. H. Chung, ''Velocity distributions in magnetron sputter,'' *IEEE Trans. Plasma Sci.*, vol. 26, pp. 1635–1644, 1998.
[21] H. J. Lee, J. K. Lee, M. S. Hur, and Y. Yang, ''A universal characterization of nonlinear self-oscillation and chaos in various particle-wave-wall interactions,'' *Appl. Phys. Lett.*, vol 72, pp. 1445–1447, 1998.
[22] H. J. Lee and J. K. Lee, "Mode transition and nonlinear self-oscillations in the beam-driven collisional discharge plasma," *Phys. Plasmas*, vol 5, pp. 2878–2884 Aug. 1998.
[23] M. S. Hur, H. J. Lee, and J. K. Lee, ''Parameterization of nonlinear and chaotic oscillations in driven beam-plasma diodes,'' *Phys. Rev. E.*, vol 58, pp. 936–941, 1998.

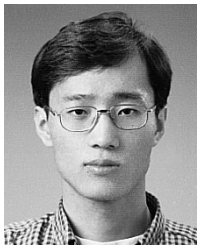

Young Kyo Shin received the B.S. degree in physics engineering from the Sung Kyun Kwan University in 1995 and the M.S. degree in physics from Pohang University of Science and Technology (POSTECH), South Korea, in 1997. He is currently working toward the Ph.D. degree at POSTECH.

His current research interests are in plasma display panels.

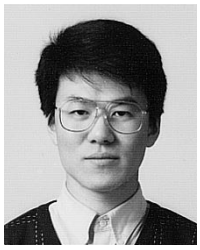

Chae Hwa Shon received the B.S. degree in nuclear engineering from the Seoul National University, Korea, in 1991, the M.S. degree in physics from the Pohang University of Science and Technology (POSTECH), South Korea, 1996. He is currently working toward the Ph.D. degree at POSTECH.

His current research interests are plasma display panels and magnetron sputter system. He is also studying electron and ion energy distributions of the above systems.

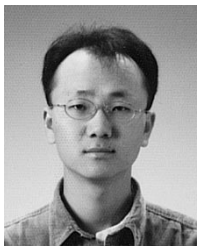

Woong Kim received the B.S. degree in physics and the M.S. degree in physics from the Pohang University of Science and Technology (POSTECH) in 1997 and 1999, respectively. He is currently working toward the Ph.D. degree at POSTECH.

His current research interest is on plasma display panels (PDP's). He is also developing a hybrid code (electron particle and ion fluid) for the PDP systems.

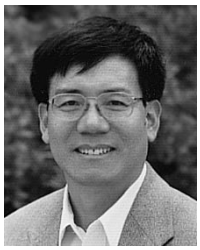

Jae Koo Lee received the Ph.D. degree from the University of California, Berkeley in 1979.

From 1979 to 1989, he worked at General Atomics, San Diego, CA as a Senior (later as a Staff) Scientist on tokamak theory. In 1989, he moved to the Physics Department of Pohang University of Science and Technology as a Professor. His research interests are the theory and simulation of low-temperature basic/processing plasmas, fusion plasmas, and free-electron lasers.

Dr. Lee is currently the Chair of Division of Plasma Physics of Korean Physical Society.